Exact Time-dependent Solutions for the Thin Accretion Disc Equation: Boundary Conditions at Finite Radius

Takamitsu Tanaka

Department of Astronomy, Columbia University, 550 West 120th Street, New York, NY 10027

ABSTRACT

We discuss Green's-function solutions of the equation for a geometrically thin, axisymmetric Keplerian accretion disc with a viscosity prescription $\nu \propto R^n$. The mathematical problem was solved by Lynden-Bell & Pringle (1974) for the special cases with boundary conditions of zero viscous torque and zero mass flow at the disc center. While it has been widely established that the observational appearance of astrophysical discs depend on the physical size of the central object(s), exact time-dependent solutions with boundary conditions imposed at finite radius have not been published for a general value of the power-law index n. We derive exact Green's-function solutions that satisfy either a zero-torque or a zero-flux condition at a nonzero inner boundary $R_{\rm in} > 0$, for an arbitrary initial surface density profile. Whereas the viscously dissipated power diverges at the disc center for the previously known solutions with $R_{\rm in} = 0$, the new solutions with $R_{\rm in} > 0$ have finite expressions for the disc luminosity that agree, in the limit $t \to \infty$, with standard expressions for steady-state disc luminosities. The new solutions are applicable to the evolution of the innermost regions of thin accretion discs.

Subject headings: accretion, accretion discs

1. Introduction

Since its emergence in the 1970's (Shakura & Sunyaev 1973; Novikov & Thorne 1973; Lynden-Bell & Pringle 1974), the theory of astrophysical accretion discs has been applied to explain the emission properties of active galactic nuclei, X-ray binaries, cataclysmic binaries, supernovae, gamma-ray bursts, and the electromagnetic signatures of mergers of supermassive black holes; to study planetary and star formation; and to model the evolution of binary and planetary systems. Because accretion discs onto compact objects can dissipate

much larger fractions of baryonic rest-mass energies than nuclear reactions, they are often associated with some of the most energetic astrophysical processes in the universe.

If the local gravitational potential is dominated by a central compact object or a compact binary, and if the timescale for the viscous dissipation of energy is longer than the orbital timescale, then the accretion flow near the center of the potential is expected to be nearly axisymmetric. If the gas is able to cool efficiently, then the flow will also be geometrically thin, and one only needs the radial coordinate to describe the mass distribution in the disc (any relevant vertical structure can be integrated or averaged over the disc height). The partial differential equation (Lynden-Bell & Pringle 1974, henceforth LP74)

$$\frac{\partial}{\partial t}\Sigma(R,t) = \frac{1}{R}\frac{\partial}{\partial R}\left[R^{1/2}\frac{\partial}{\partial R}\left(3\nu\Sigma R^{1/2}\right)\right], \tag{1}$$

is obtained by combining the equations of mass conservation and angular momentum, and describes the surface density evolution of a thin Keplerian accretion disc due to kinematic viscosity ν.

In general, the viscosity ν depends on the surface density Σ and equation (1) is nonlinear. If, however, ν is only a function of radius, then the equation is linear and much more amenable to analytic methods. In particular, a solution that makes use of a Green's function G,

$$\Sigma(R,t) = \int_{R_{\rm in}}^{\infty} G(R,R',t)\ \Sigma(R',t=0)\ dR', \tag{2}$$

gives the solution Σ for any $t > 0$ given an arbitrary profile $\Sigma(R, t = 0)$ and an inner boundary condition imposed at $R_{\rm in}$. A distinct advantage of the formalism is that it gives the solution $\Sigma(R,t)$ through a single ordinary integral, whereas a finite-difference algorithm would require the computation of the profile at intermediate times. Another advantage is that the initial density profile need not be differentiable.

For a power-law viscosity $\nu \propto R^n$, Lüst (1952) and LP74 derived analytic Green's functions that satisfy a boundary condition of either zero-torque or zero-mass-flux at the coordinate origin, i.e., for the case $R_{\rm in} = 0$. In reality, however, the objects at the center of astrophysical accretion discs have a finite size to which the observational appearance of the disc is sensitive: e.g., the luminosity, spectral hardness, and variability timescales of black hole discs depend strongly on the radius of the innermost stable orbit, and those of circumbinary discs depend on where the inner disc is truncated by the central tidal torques. Green's functions with $R_{\rm in} = 0$ do not capture the time-dependent behavior of accretion discs close to the central object. In fact, in solutions obtained with such Green's functions, the integral for the total power viscously dissipated in the center of the disc diverges.

Despite the astrophysical relevance of Green's functions to the thin accretion disc equation with boundary conditions imposed at a finite radius, such solutions have not been published. Pringle (1991) derived the Green's function with a zero-flux boundary condition at a nonzero radius in the special case $n = 1$, and noted the "extreme algebraic complexity" involved in calculating a more general solution with $R_{\rm in} > 0$. Time-dependent models of accretion flows have continued to employ solutions that correspond to the central objects having zero physical size (e.g., Metzger et al. 2008; Tanaka & Menou 2010). In order to calculate a convergent disc luminosity and spectrum, such models typically approximate analytically the effects of an inner boundary condition, e.g., by truncating the disc profile at an artificially imposed radius.

In this paper we derive exact Green's functions for equation (1) for boundary conditions imposed at a finite radius, for any power-law viscosity $\nu \propto R^n$ with $n < 2$. We show that mathematical difficulties can be minimized with the aid of the appropriate integral transform techniques, namely the Weber transform (Titchmarsh 1923) and the recently proved generalized Weber transform (Zhang & Tong 2007). We present two specific solutions of astrophysical interest: the solution with zero torque at a radius $R_{\rm in} > 0$, which is of interest for accretion discs around black holes and slowly rotating stars; and the solution with zero mass flow at $R_{\rm in} > 0$, which is applicable to accretion flows that accumulate mass at the disc center due to the injection of angular momentum from the tidal torques of a binary or perhaps the strong magnetic field of the central object.

This paper is organized as follows. In §2, we review the Green's function solutions, derived by Lüst (1952) and LP74, for the thin-disc equation with boundary conditions imposed at the origin. In §3, we derive the new Green's function solutions, which impose boundary conditions at a finite inner boundary radius. We offer our conclusions in §4.

2. Green's-Function Solutions with Boundary Conditions at $R = 0$

In the special case where the viscosity is a radial power law, $\nu \propto R^n$, and assuming a separable ansatz of the form $\Sigma(R,t) = R^p \sigma(R) \exp(-\Lambda t)$, where p and Λ are real numbers and σ is an arbitrary function of R, equation (1) can be rewritten as the Bessel differential equation:

$$R^2 \frac{\partial^2 \sigma}{\partial R^2} + \left(2p + 2n + \frac{3}{2}\right) R \frac{\partial \sigma}{\partial R} + \left[(p+n)\left(\frac{\Lambda}{3s} R^{2-n} + p + n + \frac{1}{2}\right)\right] \sigma = 0. \qquad (3)$$

Above, $s = \nu R^{-n}$ is a constant. With the choices $p = n - 1/4$ and $\Lambda = 3sk^2$, equation (3) has the general solution

$$\sigma_k(R) = R^{-2n} \left[A(k) J_\ell(ky) + B(k) Y_\ell(ky) \right]. \tag{4}$$

Above, k is an arbitrary mode of the solution; $A(k)$ and $B(k)$ are the mode weights; $\ell = (4-2n)^{-1} > 0$; $y(R) \equiv R^{(1-n/2)}/(1-n/2)$; and J_ℓ and Y_ℓ are the Bessel functions of the first and second kinds, respectively, and of order ℓ. If ℓ is not an integer, then Y_ℓ above may be replaced without loss of generality by $J_{-\ell}$. Integrating the fundamental solution across all possible k-modes gives the solution:

$$\Sigma(R,t) = \int_0^\infty R^{-n-1/4} \left[A(k) J_\ell(ky) + B(k) Y_\ell(ky) \right] \ \exp(-3sk^2 t) \ dk. \tag{5}$$

The mode-weighting functions $A(k)$ and $B(k)$ are determined by the boundary conditions and the initial surface density profile $\Sigma(R, t = 0)$. Our goal is to rewrite equation (5) in the Green's function form (equation 2) and to write down an explicit symbolic expression for the Green's function $G(R, R', t)$. Throughout this paper, we will employ the following strategy:

1. Using the boundary condition, find an analytic relationship between the mode weights $A(k)$ and $B(k)$.
2. Identify the appropriate integral transform to express the mode weights in terms of the initial profile $\Sigma(R, t = 0)$.
3. Insert the time-dependence $\exp(-3sk^2 t)$ and integrate over all modes to find the Green's function.
4. Derive analytic expressions for the asymptotic disc behavior at late times and small radii.

Before deriving the solutions with boundary conditions at finite radius, we begin by reviewing the Green's functions of LP74 with boundary conditions at the coordinate origin.

2.1. Zero torque at $R_{\rm in} = 0$

An inner boundary condition with zero central torque is of astrophysical interest as it can be used to describe accretion onto a black hole or a slowly rotating star, at radii much

larger than the radius of innermost circular orbit or the stellar surface, respectively. The radial torque density g in the disc due to viscous shear is

$$g(R,t) = \nu\Sigma R^2 \frac{\partial\Omega_{\rm K}}{\partial R} \propto \nu\Sigma R^{1/2}, \tag{6}$$

where $\Omega_{\rm K}$ is the Keplerian angular velocity of the orbit.

Because the functions J_ℓ and Y_ℓ have the asymptotic behaviors $J_\ell(ky) \propto y^\ell \propto R^{1/4}$ and $Y_\ell(ky) \propto y^{-\ell} \propto R^{-1/4}$ near the origin, at small radii the mode weight $A(k)$ will contribute to the behavior $g \propto R^{1/2}$ while $B(k)$ will contribute to $g =$ constant. Therefore, for the solution to have zero viscous torque at $R = 0$ the function $B(k)$ must be identically zero.

We may relate the surface density distribution at $t = 0$ and the weight $A(k)$ via the integral equation

$$\Sigma(R, t = 0) = R^{-n-1/4} \int_0^\infty A(k) J_\ell(ky)\, dk, \tag{7}$$

which may be solved with the use of the Hankel integral transform (e.g., Ogilvie 2005).

A Hankel transform pair of order ℓ satisfies

$$\phi_\ell(x) = \int_0^\infty \Phi_\ell(k)\ J_\ell(kx)\ k\ dk, \tag{8}$$

$$\Phi_\ell(k) = \int_0^\infty \phi_\ell(x)\ J_\ell(kx)\ x\ dx. \tag{9}$$

For the problem at hand, the suitable transform pair is

$$R^{n+1/4}\Sigma(R, t = 0) = \int_0^\infty \left[A(k)k^{-1}\right] J_\ell(ky)\ k\ dk, \tag{10}$$

$$A(k)k^{-1} = \int_0^\infty \left[R^{n+1/4}\Sigma(R, t = 0)\right] J_\ell(ky)\ y\ dy. \tag{11}$$

Combining them gives us $A(k)$:

$$A(k) = \left(1 - \frac{n}{2}\right)^{-1} \int_0^\infty \Sigma(y', 0)\ J_\ell(ky')\ k\ R'^{5/4}\ dR' \tag{12}$$

Inserting equation (12) and $B(k) = 0$ into equation (5), we obtain

$$\Sigma(R,t) = \left(1 - \frac{n}{2}\right)^{-1} R^{-n-1/4} \int_0^\infty R'^{5/4} \int_0^\infty \Sigma(R', t = 0)\ J_\ell(ky')\ J_\ell(ky)\ \exp\left(-3sk^2t\right)\ k\ dk\ dR'. \tag{13}$$

To pose the solution in terms of a Green's function $G(R, R', t)$ (equation 2), we write

$$G(R, R', t) = \left(1 - \frac{n}{2}\right)^{-1} R^{-n-1/4} R'^{5/4} \int_0^\infty J_\ell(ky')\ J_\ell(ky)\ \exp\left(-3sk^2 t\right)\ k\ dk$$
$$= (2-n)\frac{R^{-9/4} R'^{5/4}}{\tau(R)} I_\ell \left[\frac{2\,(R'/R)^{1-n/2}}{\tau(R)}\right] \exp\left[-\frac{1 + (R'/R)^{2-n}}{\tau(R)}\right]. \qquad (14)$$

Above, I_ℓ is the modified Bessel function of the first kind, and we have substituted $\tau(R) \equiv 12(1-n/2)^2 R^{n-2} st = 8(1-n/2)^2[t/t_\nu(R)]$, where $t_\nu(R) = (2/3)R^2/\nu(R)$ is the local viscous timescale at R.

Although the Green's function allows for the calculation of $\Sigma(R, t)$ for arbitrary initial surface density profiles, it is instructive to study the case where the initial surface density is a Dirac δ function,

$$\Sigma(R, t = 0) = \Sigma_0\ \delta(R - R_0)\ R_0, \qquad (15)$$

for which the solution is (by definition) the Green's function itself. The integral over radius in equation (2) becomes trivial and many behaviors of the solution may be expressed analytically. Because any initial surface density profile can be described as a superposition of δ-functions, studying this special case will help illuminate the general behavior of all solutions.

We may evaluate the asymptotic behavior at late times and small radii by noting that for small argument $z \lesssim 0.2\sqrt{1+\ell}$, $I_\ell(z) \approx (z/2)^\ell/\Gamma(\ell+1)$. We find

$$\Sigma\left(R, t \gtrsim t_\nu(R)\right) \approx \frac{2-n}{\Gamma(\ell+1)} \Sigma_0 \left(\frac{R}{R_0}\right)^{-n} \left[8\left(1 - \frac{n}{2}\right)^2 \frac{t}{t_{\nu,0}}\right]^{-1-\ell}, \qquad (16)$$

where $t_{\nu,0} \equiv t_\nu(R_0)$.

Thus, for these solutions the inward radial mass flow,

$$\dot{M}(R) = -2\pi R \Sigma v_R = 6\pi R^{1/2} \frac{\partial}{\partial R}\left(\nu \Sigma R^{1/2}\right), \qquad (17)$$

becomes radially constant near the origin and at late times:

$$\dot{M}\left(t \gtrsim t_\nu(R)\right) \approx \frac{2-n}{\Gamma(\ell+1)} \dot{M}_0 \left[8\left(1 - \frac{n}{2}\right)^2 \frac{t}{t_{\nu,0}}\right]^{-1-\ell}. \qquad (18)$$

Above, we have defined $\dot{M}_0 \equiv 3\pi\nu(R_0)\Sigma_0$.

The power per unit area that is locally viscously dissipated from each face of the disc is $F = (9/8)\nu\Sigma\Omega^2$. The total power dissipated near the center of the disc diverges:

$$L\left(R, t \gtrsim t_\nu(R)\right) = \int_0^R \frac{9\pi}{2} \nu(R')\Sigma(R', t)\Omega^2(R') R'\ dR' \propto \int_0^R R'^{-2}\ dR'. \qquad (19)$$

Astrophysical accretion flows do not extend to zero radius, and thus in practice one may truncate the disc at some plausible boundary radius, for example the radius of innermost stable circular orbit for a disc around a black hole, by approximating the effects of a finite boundary radius (LP74).

Although we have used a δ function for demonstrative purposes, the quantities R_0 and Σ_0 that set the physical scale and normalization of the initial surface density profile, respectively, are arbitrary. The asymptotic behaviors noted above hold for any initial surface density profile: at late times, the surface density profile approaches $\Sigma \propto R^{-n}$, $\dot{M}$ becomes radially constant, and the disc luminosity L formally diverges at the center.

At early times and large radii, such that $t \ll \sqrt{t_\nu(R)\ t_\nu(R')}$, we may use the fact that $I_\ell(z \gg 1) \approx \exp(x)/\sqrt{2\pi z}$ to find

$$G\left(t \ll \sqrt{t_\nu(R)\ t_\nu(R')}\right) \approx \frac{1}{\sqrt{\pi\tau(R)}} \exp\left\{-\frac{\left[1-(R'/R)^{1-n/2}\right]^2}{\tau(R)}\right\} \left(\frac{R'}{R}\right)^{(3/4)(1+n)} \frac{d}{dR'}\left[\left(\frac{R'}{R}\right)'^{1-n/2}\right]. \tag{20}$$

In Figure 1, we plot the solution $\Sigma(R,t)$ and the radial mass flow $\dot{M}(R,t)$, for the δ-function initial condition (equation 15), and for viscosity power-law index values $n = 0.1$ and $n = 1$. In both cases, we see the power-law behavior from equation (16) near the origin as the solution approaches $t \sim t_{\nu,0}$. The disc spreads as the gas at inner annuli loses angular momentum to the gas at outer annuli. The gas initially accumulates near the origin, then becomes diffuse as mass is lost into the origin.

2.2. Zero mass flow at $R_{\rm in} = 0$

If the accretion flow has a sufficiently strong central source of angular momentum, then the gas will be unable to flow in, and instead accumulate near the origin. Such solutions can be used to describe astrophysical discs around a compact binary (Pringle 1991), and perhaps those around compact objects with strong central magnetic fields (LP74). For circumbinary thin discs, Pringle (1991) demonstrated that such a boundary condition characterizes quite well the effects of an explicit central torque term.

In general, the mass flow has the behavior

$$\dot{M} \propto \int_0^\infty R^{1/2} \frac{\partial}{\partial R}\left[A(k) J_\ell(ky) R^{1/4} + B(k) Y_\ell(ky) R^{1/4}\right]\ \exp(-3sk^2 t)\ dk. \tag{21}$$

We have seen above that for solutions with $B(k) = 0$ the mass flow is radially constant

and finite near the origin. On the other hand, because $Y_\ell(ky) \propto R^{-1/4}$ near the origin, the weights $B(k)$ will all contribute no mass flow there; so for zero mass flow at $R_{\rm in} = 0$, we require $A(k) = 0$.

We note that because the surface density will have a power-law $\Sigma \propto R^{-1/2-n}$ at the origin, for the mass contained in the disc to converge n must be less than 3/2. Thus, for physically realistic solutions with zero mass flow at the origin, ℓ cannot be an integer. It follows that in this case Y_ℓ in equation (5) may be replaced by $J_{-\ell}$ without loss of generality. Then the Green's function for this case is derived in exactly the same fashion as in the previous case, the only difference being that the order of the Hankel transforms has the opposite sign. We obtain:

$$G(R, R', t) = (2-n)\frac{R^{-9/4}R'^{5/4}}{\tau(R)} I_{-\ell}\left[\frac{2\left(R'/R\right)^{1-n/2}}{\tau(R)}\right] \exp\left[-\frac{1+\left(R'/R\right)^{2-n}}{\tau(R)}\right]. \tag{22}$$

As before, we evaluate the late-time behavior for the δ-function initial condition (equation 15) at small radii:

$$\Sigma\left(R, t \gtrsim t_\nu(R)\right) \approx \frac{2-n}{\Gamma(1-\ell)}\Sigma_0 \left(\frac{R}{R_0}\right)^{-n-1/2} \left[8\left(1-\frac{n}{2}\right)^2 \frac{t}{t_{\nu,0}}\right]^{-1+\ell}. \tag{23}$$

From the above expression it is clear that the boundary condition is satisfied: $\dot{M} \propto \partial(\nu\Sigma R^{1/2}) \to 0$ in the limit $R \to 0$. Just as we found for the zero-torque boundary condition, the formal expression for the power dissipated at the disc center diverges for the zero-flux solution, with $L(R \leq R_0, t \gtrsim t_{\nu,0}) \propto \int_0^{R_0} R^{-5/2}\, dR$.

The asymptotic behavior at early times and large radii is unaffected by the order of the function I_ℓ; it is described by equation 20. Indeed, the inner boundary condition should have no effect on the disc at large radii.

Figure 2 shows the evolution of the surface density and the radial mass flow for the boundary condition $\dot{M}(R = 0) = 0$. At early times, the behavior is nearly identical to the zero-torque boundary case. At late times, the zero-flux boundary condition causes the gas to accumulate instead of being lost to the origin. The central mass concentration reaches a maximum, then decreases as the disc begins to spread outward.

3. Green's-Function Solutions with Boundary Conditions at Finite Radii

As we have seen above, Green's-function solutions of thin accretion discs with $R_{\rm in} = 0$ have divergent expressions for the dissipated power, and thus the innermost surface density profile must be manipulated to obtain physically realistic disc luminosities. Analytic

treatment of the case with finite boundary radius was briefly discussed in LP74 and Pringle (1991), but to the author's knowledge explicit solutions have never before been published. We show below that the Green's functions for finite boundary radii can be derived with the aid of the appropriate integral transform techniques, and that they can be represented as ordinary integrals of analytic functions.

3.1. Zero Torque at $R_{\rm in} > 0$

We wish to solve the problem as in §2.1, but with $R_{\rm in} > 0$, i.e.

$$g(R_{\rm in}) \propto \Sigma\nu R^{1/2}\Big|_{R=R_{\rm in}} \propto \Sigma(R_{\rm in})R_{\rm in}^{n+1/2} = 0. \tag{24}$$

We may relate the mode weights $A(k)$ and $B(k)$ by requiring that every mode of the solution satisfy the boundary condition, i.e.:

$$A(k)J_\ell(ky_{\rm in}) + B(k)Y_\ell(ky_{\rm in}) = 0, \tag{25}$$

where $y_{\rm in} \equiv y(R_{\rm in})$. Substituting $C(k) = A(k)/Y_\ell(ky_{\rm in}) = -B(k)/J_\ell(ky_{\rm in})$, we obtain

$$\Sigma(R,t) = \int_0^\infty C(k)R^{-n-1/4}\left[J_\ell(ky)Y_\ell(ky_{\rm in}) - Y_\ell(ky)J_\ell(ky_{\rm in})\right]\exp(-3sk^2t)\ dk. \tag{26}$$

The function $C(k)$ may be evaluated with the use of the Weber integral transform (Titchmarsh 1923). A Weber transform pair satisfies

$$\phi_\ell(x) = \int_0^\infty \Phi_\ell(\kappa)\frac{J_\ell(\kappa x)Y_\ell(\kappa) - Y_\ell(\kappa x)J_\ell(\kappa)}{J_\ell^2(\kappa) + Y_\ell^2(\kappa)}\ \kappa\ d\kappa, \tag{27}$$

$$\Phi_\ell(\kappa) = \int_1^\infty \phi_\ell(x)\left[J_\ell(\kappa x)Y_\ell(\kappa) - Y_\ell(\kappa x)J_\ell(\kappa)\right]\ x\ dx. \tag{28}$$

Proceeding as before, we construct the pair

$$R^{n+1/4}\Sigma(R,t=0) = \int_0^\infty \left[C(\kappa)\kappa^{-1}\right]\frac{J_\ell(\kappa x)Y_\ell(\kappa) - Y_\ell(\kappa x)J_\ell(\kappa)}{J_\ell^2(\kappa) + Y_\ell^2(\kappa)}\ \kappa\ d\kappa, \tag{29}$$

$$C(\kappa)\kappa^{-1} = \int_1^\infty \left[R^{n+1/4}\Sigma(R,t=0)\right]\left[J_\ell(\kappa x)Y_\ell(\kappa) - Y_\ell(\kappa x)J_\ell(\kappa)\right]\ x\ dx. \tag{30}$$

Above, we have substituted $x = y/y_{\rm in} \geq 1$ and $\kappa = ky_{\rm in}$. Note the lower limit of integration in equation (30) is nonzero to account for the finite boundary radius. Combining equations (29) and (30) to eliminate $C(\kappa)$, and inserting the time-dependence factor

$\exp(-3sk^2t) = \exp[-2(1-n/2)^2\kappa^2 t/t_{\nu,\rm in}]$ where $t_{\nu,\rm in} = t_\nu(R_{\rm in})$, we obtain our new Green's function:

$$G(R,R',t) = \left(1-\frac{n}{2}\right) R^{-n-1/4} R'^{5/4} R_{\rm in}^{n-2} \times \int_0^\infty \frac{[J_\ell(\kappa x)Y_\ell(\kappa) - Y_\ell(\kappa x)J_\ell(\kappa)]\,[J_\ell(\kappa x')Y_\ell(\kappa) - Y_\ell(\kappa x')J_\ell(\kappa)]}{J_\ell^2(\kappa)+Y_\ell^2(\kappa)} \times \exp\left[-2\left(1-\frac{n}{2}\right)^2 \kappa^2 \frac{t}{t_{\nu,\rm in}}\right]\ \kappa\ d\kappa. \tag{31}$$

Whereas the integral over k in equation (14) has an analytic solution, to the author's knowledge there is no analytic expression for the integral in equation (31). Nonetheless, equation (31) gives an exact expression for the Green's function. While it is somewhat more unwieldy than the solutions for $R_{\rm in} = 0$, the additional computational cost of an ordinary integral is not likely to be a significant practical barrier, e.g. one could tabulate the integral in terms of the quantities x, x' and $t/t_{\nu,\rm in}$. The boundary condition has little effect at large radii, so in practice the behavior far from the boundary is well approximated by the $R_{\rm in} = 0$ solutions.

The Green's function in equation (14) does have a closed-form expression for the special case $n = 1$ (i.e., $\ell = 1/2$). As noted by Pringle (1991), in this case the Bessel functions become easier to handle analytically, with $J_{1/2}(x) = \sqrt{\pi/2}\ x^{-1/2}\sin x$ and $Y_{1/2}(x) = -\sqrt{\pi/2}\ x^{-1/2}\cos x$. For this value of n we obtain for our Green's function

$$\begin{aligned} G(R,R',t) &= \frac{1}{\pi R_{\rm in}}\left(\frac{R'}{R}\right)^{5/4} (x\ x')^{-1/2} \int_0^\infty \sin\left[\kappa(x-1)\right]\sin\left[\kappa(x'-1)\right]\ \exp\left[-\frac{\kappa^2}{2}\frac{t}{t_{\nu,\rm in}}\right]\ d\kappa \\ &= \frac{R^{-3/2}R'R_{\rm in}^{-1/2}}{2\sqrt{2\pi}}\sqrt{\frac{t_{\nu,\rm in}}{t}}\left\{\exp\left[-\frac{(x-x')^2}{2}\frac{t}{t_{\nu,\rm in}}\right] - \exp\left[-\frac{(x+x'-2)^2}{2}\frac{t}{t_{\nu,\rm in}}\right]\right\}. \end{aligned} \tag{32}$$

Note that in the case $n = 1$, x and x' are simply $\sqrt{R/R_{\rm in}}$ and $\sqrt{R'/R_{\rm in}}$, respectively.

For general values of n, we can evaluate the behavior at late times $t \gtrsim t_{\nu,0} > t_{\nu,\rm in}$ by noting that in this regime only the modes $\kappa^2 \lesssim 1$ contribute to the integral in equation (31). For the central region $R \lesssim R_0$ at late times, we obtain the following analytic expression for

the δ-function initial condition:

$$\Sigma\left(R, t \gtrsim t_\nu(R)\right) \approx \frac{2-n}{2^{1+2\ell}\Gamma^2(1+\ell)}\Sigma_0 \left(\frac{R}{R_{\rm in}}\right)^{-n} \left(\frac{R_0}{R_{\rm in}}\right)^{5/2} \left(1-\sqrt{\frac{R_{\rm in}}{R}}\right)\left(\sqrt{\frac{R_0}{R_{\rm in}}}-1\right) \times \int_0^\infty \exp\left[-2\left(1-\frac{n}{2}\right)^2 \kappa^2 \frac{t}{t_{\nu,{\rm in}}}\right] \kappa^{1+2\ell}\, d\kappa$$
$$= \frac{2-n}{\Gamma(1+\ell)}\Sigma_0 \left(\frac{R}{R_{\rm in}}\right)^{-n} \left(\frac{R_0}{R_{\rm in}}\right)^{5/2} \left(1-\sqrt{\frac{R_{\rm in}}{R}}\right)\left(\sqrt{\frac{R_0}{R_{\rm in}}}-1\right) \left[8\left(1-\frac{n}{2}\right)^2 \frac{t}{t_{\nu,{\rm in}}}\right]^{-1-\ell}. \quad (33)$$

We see that the Green's function explicitly gives the asymptotic behavior $\Sigma \propto R^{-n}(1-\sqrt{R_{\rm in}/R})$, which has been used extensively for solutions of accretion discs near zero-torque boundary surfaces (e.g., LP74, Frank et al. 2002).[1] This behavior near the boundary and at late times is general for any initial surface density profile; it is insensitive to the values of Σ_0 and R_0, and arises for any nonzero $R_{\rm in}$. This qualitative difference in the inner disc from the $R_{\rm in} = 0$ case also gives a convergent value for the power dissipated in the central disc. We obtain:

$$L\left(R \leq R_t, t \gtrsim t_\nu(R)\right) = \frac{GM\dot{M}_{\rm ss}}{2R_{\rm in}}\left[1 - 3\frac{R_{\rm in}}{R_t} + 2\left(\frac{R_{\rm in}}{R_t}\right)^{3/2}\right], \quad (34)$$

where $\dot{M}_{\rm ss}$ is the mass flow quantity in equation (18), and R_t is the radius where $t = t_\nu(R)$, inside which the disc has had sufficient time to approach the asymptotic solution. In the limit $R_0 \gg R_{\rm in}$ and $t \gg t_{\nu,0}$, $\dot{M}_{\rm ss}$ may be interpreted as the mass supply rate into the center of the disc from arbitrarily large radii. In this limit the above expression agrees precisely with the standard expression for the luminosity of a steady-state thin accretion disc.

We show in Figure 3 the exact solutions for the δ-function initial condition, with the no-torque boundary condition imposed at $R_{\rm in} = R_0/5$. The qualitative evolution is as predicted by LP74: at early times, far from the boundary, the disc spreads inward in very much the same manner as the solutions with $R_{\rm in} = 0$, and so the $R_{\rm in} = 0$ Green's function suffices; at late times, once the gas reaches the vicinity of the boundary it exhibits the behavior $\Sigma \propto R^{-n}(1-\sqrt{R_{\rm in}/R})$ in that neighborhood.

[1] The factor arises from assuming that Ω is nearly Keplerian at the radius where the torque $g \propto \partial\Omega/\partial R = 0$ (Frank et al. 2002).

3.2. Zero Mass Flux at $R_{\rm in} > 0$

We now consider the boundary condition of zero mass flow at a particular radius,

$$\dot{M}(R_{\rm in}) \propto \frac{\partial}{\partial R}\left(\nu\Sigma R^{1/2}\right)\Big|_{R=R_{\rm in}} \propto \frac{\partial}{\partial y}\left\{y^\ell\left[A(k)J_\ell(ky)+B(k)Y_\ell(ky)\right]\right\}\Big|_{y=y_{\rm in}} = 0. \tag{35}$$

From the relations $\partial[x^\ell J_\ell(x)]/\partial x = x^\ell J_{\ell-1}(x)$ and $\partial[x^\ell Y_\ell(x)]/\partial x = x^\ell Y_{\ell-1}(x)$, we obtain the relationship between A and B corresponding to the boundary condition:

$$\frac{A(\kappa)}{B(\kappa)} = -\frac{Y_{\ell-1}(\kappa)}{J_{\ell-1}(\kappa)}. \tag{36}$$

The solution is then

$$\Sigma(R,t) = \int_0^\infty C(\kappa)R^{-n-1/4}\left[J_\ell(\kappa x)\ Y_{\ell-1}(\kappa) - Y_\ell(\kappa x)\ J_{\ell-1}(\kappa)\right]\exp\left[-2\left(1-\frac{n}{2}\right)^2\kappa^2\frac{t}{t_{\nu,\rm in}}\right]\ \kappa\ d\kappa \tag{37}$$

Pringle (1991) solved the special case $n = 1$ analytically, and noted the mathematical difficulty in deriving a solution for a more general case. We find that the mode weight $C(\kappa)$ can in fact be solved for with the use of the recently proved generalized Weber transform (Zhang & Tong 2007),

$$\phi_\ell(x) = \int_0^\infty \frac{W_\ell(\kappa,x;a,b)}{Q_\ell^2(\kappa;a,b)}\ \Phi_\ell(\kappa)\ \kappa\ d\kappa, \tag{38}$$

$$\Phi_\ell(\kappa) = \int_1^\infty W_\ell(\kappa,x;a,b)\ \phi_\ell(x)\ x\ dx. \tag{39}$$

The functions $W_\ell(\kappa,x;a,b)$ and $Q_\ell^2(\kappa;a,b)$ are defined as follows:

$$\begin{aligned} W_\ell(\kappa,x;a,b) &\equiv J_\ell(\kappa x)\left[aY_\ell(\kappa)+b\kappa\ Y_\ell'(\kappa)\right] - Y_\ell(\kappa x)\left[aJ_\ell(\kappa)+b\kappa\ J_\ell'(\kappa)\right] \\ &= J_\ell(\kappa x)\left[(a-\ell b)\,Y_\ell(\kappa)+b\kappa\ Y_{\ell-1}(\kappa)\right] - Y_\ell(\kappa x)\left[(a-\ell b)\,J_\ell(\kappa)+b\kappa\ J_{\ell-1}(\kappa)\right] \end{aligned} \tag{40}$$

$$\begin{aligned} Q_\ell^2(\kappa;a,b) &\equiv \left[aY_\ell(\kappa)+b\kappa\ Y_\ell'(\kappa)\right]^2 + \left[aJ_\ell(\kappa)+b\kappa\ J_\ell'(\kappa)\right]^2 \\ &= \left[(a-\ell b)\,Y_\ell(\kappa)+b\kappa\ Y_{\ell-1}(\kappa)\right]^2 + \left[(a-\ell b)\,J_\ell(\kappa)+b\kappa\ J_{\ell-1}(\kappa)\right]^2. \end{aligned} \tag{41}$$

Above, J_ℓ' and Y_ℓ' are the ordinary derivatives of the Bessel functions. If $a = 1$ and $b = 0$, the pair is identical to the ordinary Weber transform (equations 27 and 28).

The choice $a = \ell$ and $b = 1$ corresponds to the desired boundary condition $\dot{M}(R_{\rm in},t) = 0$.

The Green's function is then:

$$G(R,R',t) = \left(1-\frac{n}{2}\right) R^{-n-1/4} R'^{5/4} R_{\rm in}^{n-2} \times \int_0^\infty \frac{\left[J_\ell(\kappa x)Y_{\ell-1}(\kappa) - Y_\ell(\kappa x)J_{\ell-1}(\kappa)\right]\left[J_\ell(\kappa x')Y_{\ell-1}(\kappa) - Y_\ell(\kappa x')J_{\ell-1}(\kappa)\right]}{J_{\ell-1}^2(\kappa)+Y_{\ell-1}^2(\kappa)} \times \exp\left[-2\left(1-\frac{n}{2}\right)^2 \kappa^2 \frac{t}{t_{\nu,\rm in}}\right] \kappa\, d\kappa. \tag{42}$$

A specific instance of the above Green's function was derived by Pringle (1991) for the case $n = 1$. We can use equation (42) to reproduce that previous solution by noting that $J_{-1/2}(x) = -Y_{1/2}(x) = \sqrt{\pi/2}\; x^{-1/2}\cos x$ and $Y_{-1/2}(x) = J_{1/2}(x) = \sqrt{\pi/2}\; x^{-1/2}\sin x$. We obtain:

$$\begin{aligned} G(R,R',t) &= \frac{1}{\pi R_{\rm in}}\left(\frac{R'}{R}\right)^{5/4} (x\;x')^{-1/2} \int_0^\infty \cos\left[\kappa(x-1)\right]\cos\left[\kappa(x'-1)\right]\;\exp\left[-\frac{\kappa^2}{2}\frac{t}{t_{\nu,\rm in}}\right]\, d\kappa \\ &= \frac{R^{-3/2}R'R_{\rm in}^{-1/2}}{2\sqrt{2\pi}}\sqrt{\frac{t_{\nu,\rm in}}{t}}\left\{\exp\left[-\frac{(x-x')^2}{2}\frac{t}{t_{\nu,\rm in}}\right] + \exp\left[-\frac{(x+x'-2)^2}{2}\frac{t}{t_{\nu,\rm in}}\right]\right\}. \end{aligned} \tag{43}$$

The only difference between this Green's function and the one for $n = 1$ and zero torque at $R_{\rm in}$ (equation 32) is the sign in between the exponential functions.

For general values of n, the analytic late-time behavior of equation (42) turns out to be identical to that for the case $R_{\rm in} = 0$ (equation 23). This can be confirmed by observing that for $\ell < 1$ and small arguments $\kappa \ll 1$ and $\kappa x \ll 1$, $W_\ell(\kappa, x; \ell, 1) \approx \csc(\ell\pi)J_{-\ell}(\kappa x)J_{\ell-1}(\kappa)$ and $Q_\ell^2(\kappa;\ell,1) \approx \csc^2(\ell\pi)J_{\ell-1}^2(\kappa)$, and therefore the large fraction in equation (42) is approximately equal to $J_{-\ell}(\kappa x)J_{-\ell}(\kappa x')$. However, because the disc does not extend to the origin for a finite boundary, the integral for the central disc luminosity converges. For the δ-function initial surface density profile, we obtain:

$$L\left(R \le R_t, t \gtrsim t_\nu(R)\right) \sim \frac{GM\dot{M}_{\rm ss}}{R_{\rm in}}\left(\sqrt{\frac{R_t}{R_{\rm in}}} - \frac{R_{\rm in}}{R_t}\right)\left[8\left(1-\frac{n}{2}\right)^2\frac{t}{t_{\nu,\rm in}}\right]^\ell, \tag{44}$$

where again $\dot{M}_{\rm ss}$ is the mass supply expression defined in §3.1, and R_t is the radius where $t = t_\nu(R)$, inside which the disc has had sufficient time to approach the asymptotic solution. The above expression for the disc luminosity is in agreement with the estimate of Ivanov et al. (1999), who considered a zero-flux boundary condition in the context of a thin disc around a supermassive black hole binary.

Figure 4 shows the solution for the δ-function initial condition and the zero-flux boundary condition at $R_{\rm in} = R_0/5$. The panels showing the mass flow clearly exhibit the desired

boundary condition. Note that the case $n = 1$ (panels b and d) is the case solved analytically by Pringle (1991). The $n = 1$ case, however, leads to a more rapid evolution and steeper late-time profiles than solutions with lower values for n; e.g., for the innermost regions of circumbinary discs around supermassive black holes, the viscosity is believed to be roughly constant with radius (Milosavljević & Phinney 2005; Tanaka & Menou 2010).

4. Conclusion

We have presented Green's functions to the equation for viscous diffusion in a thin Keplerian accretion disc, in the special case of a power-law viscosity profile $\nu \propto R^n$, for two different types of boundary conditions, zero viscous torque or zero mass flow, imposed at a finite inner radius $R_{\rm in} > 0$. They are extensions of the elegant analytic solutions derived by Lüst (1952) and LP74 for the same boundary conditions applied at $R_{\rm in} = 0$. While the problem of the finite-radius boundary had been mentioned previously in the literature, to the author's knowledge these solutions have not been explicitly pursued, and are presented here for the first time. The new solutions can be used to model the time-dependent behavior of the innermost regions of accretion discs, where the finite physical size of the central objects can significantly affect the observable characteristics of the disc. Whereas the power viscously dissipated in the $R_{\rm in} = 0$ solutions diverge, and require manipulation of the profile at the disc center to calculate physically plausible disc luminosities, the power for the new solutions converge to expressions that are consistent with disc luminosities inferred by other (non-Green's function) methods. The solutions presented here complement the numerous approximate solutions and numerical treatments in the literature.[2]

The integral transforms used to derive the solutions are applicable to a wide class of boundary conditions, and may be applicable to astrophysical thin-disc systems and configurations not considered here. Because the generalized Weber transform by its nature is applicable to many second-order differential equations with intrinsic cylindrical symmetry, they may also prove to be useful in solving other mathematical equations in astrophysics and other fields.

[2]For example, Cannizzo et al. (1990) studied the accretion of a tidally disrupted star onto a black hole via numerical solutions and analytic self-similar solutions. The problem of a thin disc with $\dot{M} = 0$ at a finite radius was discussed for the non-linear case $\nu \propto \Sigma^m \nu^n$ by Pringle (1991) and Ivanov et al. (1999), with both papers providing numerical solutions as well as analytic approximations.

Acknowledgements

It is a pleasure to thank Kristen Menou and Zoltán Haiman for helpful conversations and comments on the manuscript; and Jim Pringle and Jeremy Goodman for consultation regarding the literature. The author is also grateful to the Kavli Institute for Theoretical Physics, where a part of this work took place, for their hospitality. Support for this work was provided by NASA ATFP grant NNXO8AH35G (to KM and ZH), and also by the Polányi Program of the Hungarian National Office of Technology (to ZH).

REFERENCES

Cannizzo J. K., Lee H. M., Goodman J., 1990, ApJ, 351, 38

Frank J., King A., Raine D. J., 2002, Accretion Power in Astrophysics: Third Edition. Cambridge University Press

Ivanov P. B., Papaloizou J. C. B., Polnarev A. G., 1999, MNRAS, 307, 79

Lüst R., 1952, Z.Naturforsch, 7a, 87

Lynden-Bell D., Pringle J. E., 1974, MNRAS, 168, 603 (LP74)

Metzger B. D., Piro A. L., Quataert E., 2008, MNRAS, 390, 781

Milosavljević M., Phinney E. S., 2005, ApJ, 622, L93

Novikov I. D., Thorne K. S., 1973, in Black Holes (Les Astres Occlus) Astrophysics of black holes.. pp 343–450

Ogilvie G. I., , 2005, Unpublished lecture notes on "Accretion Discs", `http://www.damtp.cam.ac.uk/user/gio10/lecture5.pdf`

Pringle J. E., 1991, MNRAS, 248, 754

Shakura N. I., Sunyaev R. A., 1973, A&A, 24, 337

Tanaka T., Menou K., 2010, ApJ, 714, 404

Titchmarsh E. C., 1923, Proc. London Math. Soc. (2), 22, 15

Zhang X., Tong D., 2007, Applied Mathematics and Computation, 193, 116

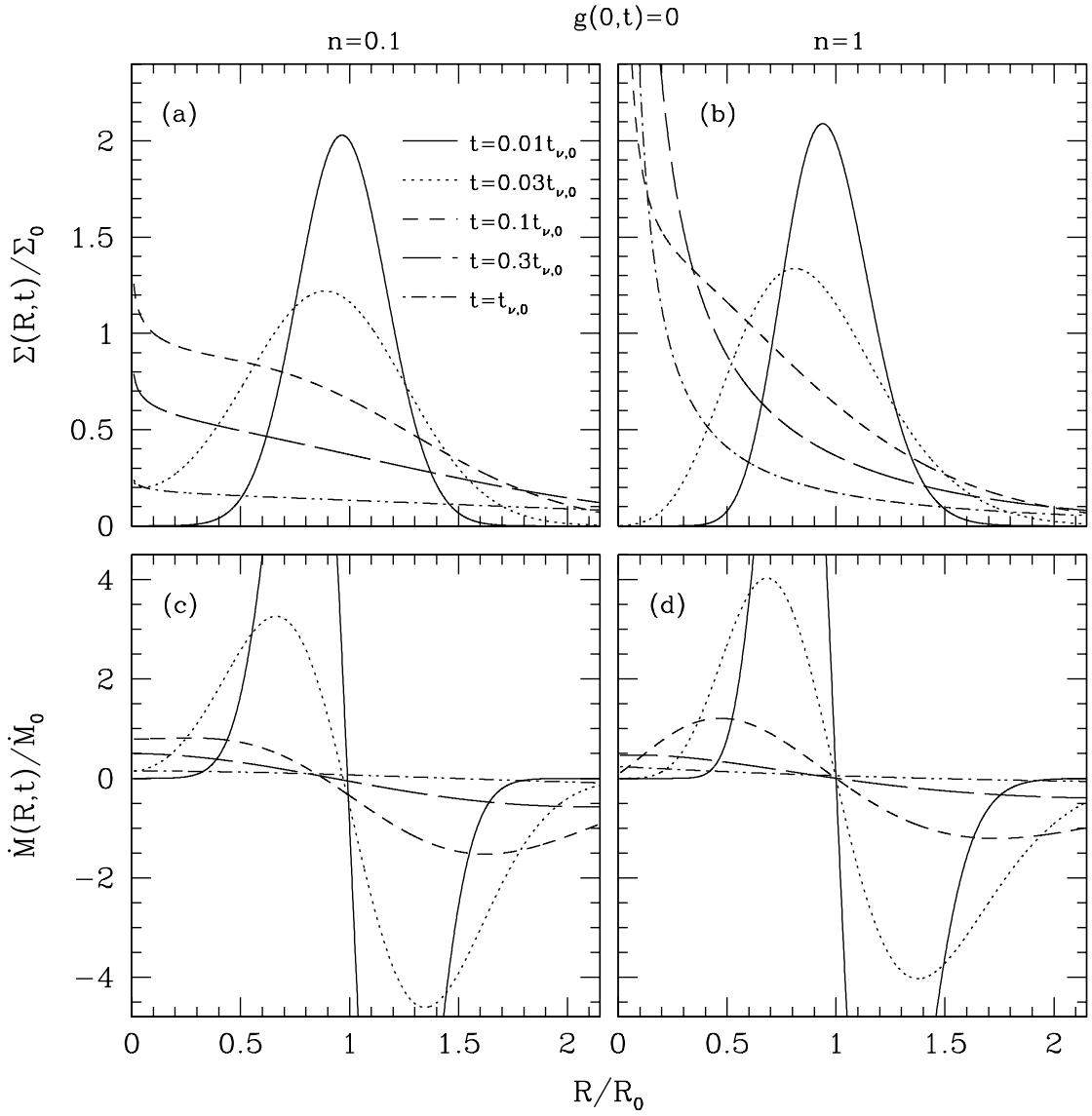

Fig. 1.— The solution $\Sigma(R,t)$, from LP74, and the corresponding radial mass inflow rate $\dot{M}(R,t)$, for a zero-torque boundary condition imposed at $R = 0$ and a δ-function initial profile $\Sigma(R, t = 0) = \Sigma_0 R_0 \delta(R - R_0)$, where the quantities Σ_0 and R_0 are arbitrary. The viscosity is a radial power law with $\nu \propto R^n$. Panels on the left side (a and c) show solutions for $n = 0.1$, and those on the right (b and d) show solutions for $n = 1$. Values for t are in units of the viscous time at R_0, $t_{\nu,0} = (2/3)R_0^2/\nu(R_0)$. We have normalized $\dot{M}$ to the quantity $\dot{M}_0 \equiv 3\pi\nu(R_0)\Sigma_0$. At late times, the solution has the behavior $\Sigma \propto R^{-n}$ and the mass-flow profile $\dot{M}$ becomes flat near the origin.

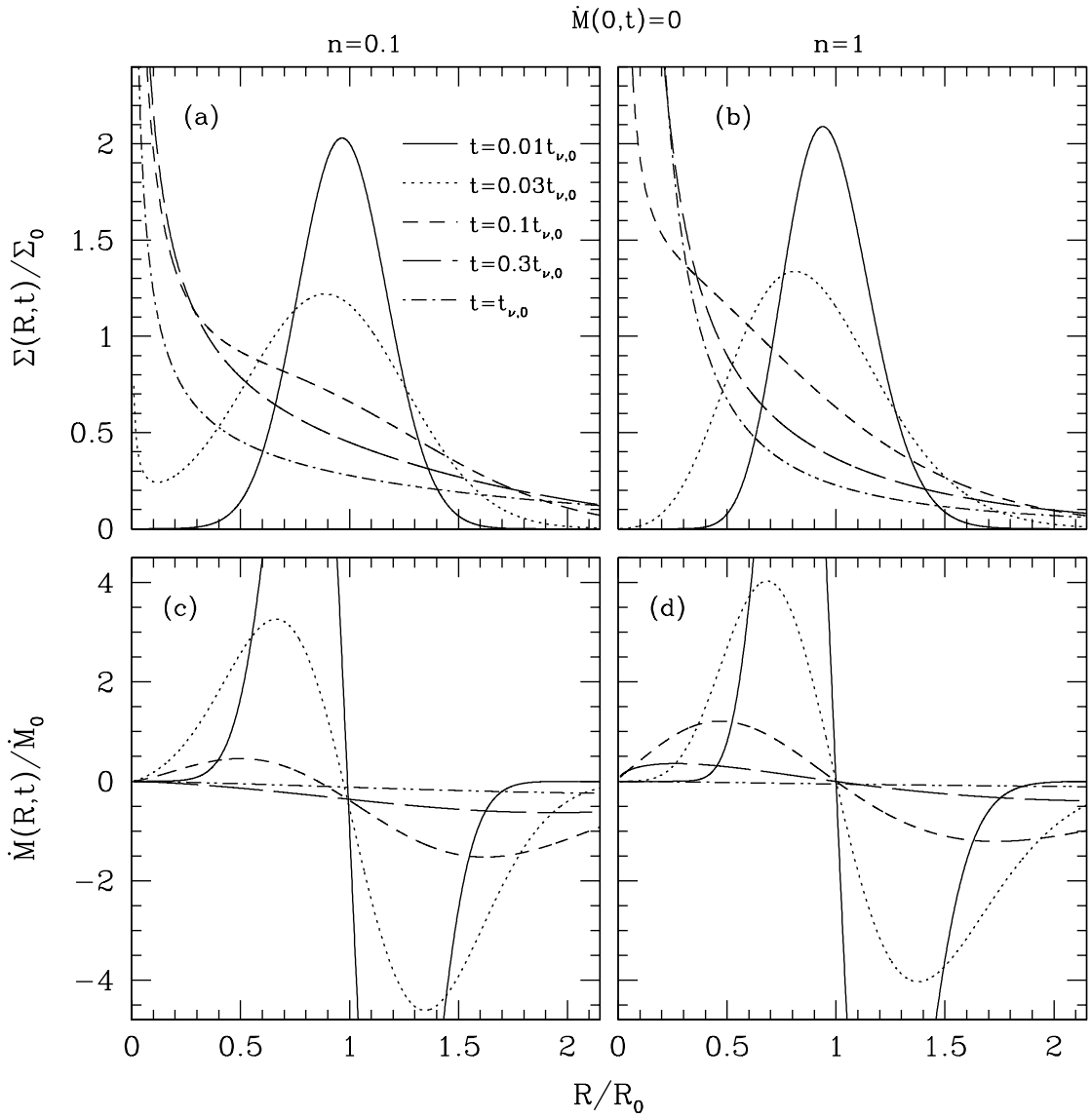

Fig. 2.— Same as Figure 1, except that the boundary condition is $\dot{M} = 0$ at $R = 0$. Again, the scales Σ_0 and R_0 are arbitrary. Whereas in the zero-torque case the total mass in the disc monotonically decreases due to mass loss at the origin (onto the black hole or star), the solutions in this figure conserve mass. At late times, the solution has the behavior $\Sigma \propto R^{-n-1/2}$. Gas initially piles up near the origin because of the boundary condition before gradually spreading outward; note that Σ at inner radii decreases from $t = 0.3t_{\nu,0}$ to $t = t_{\nu,0}$.

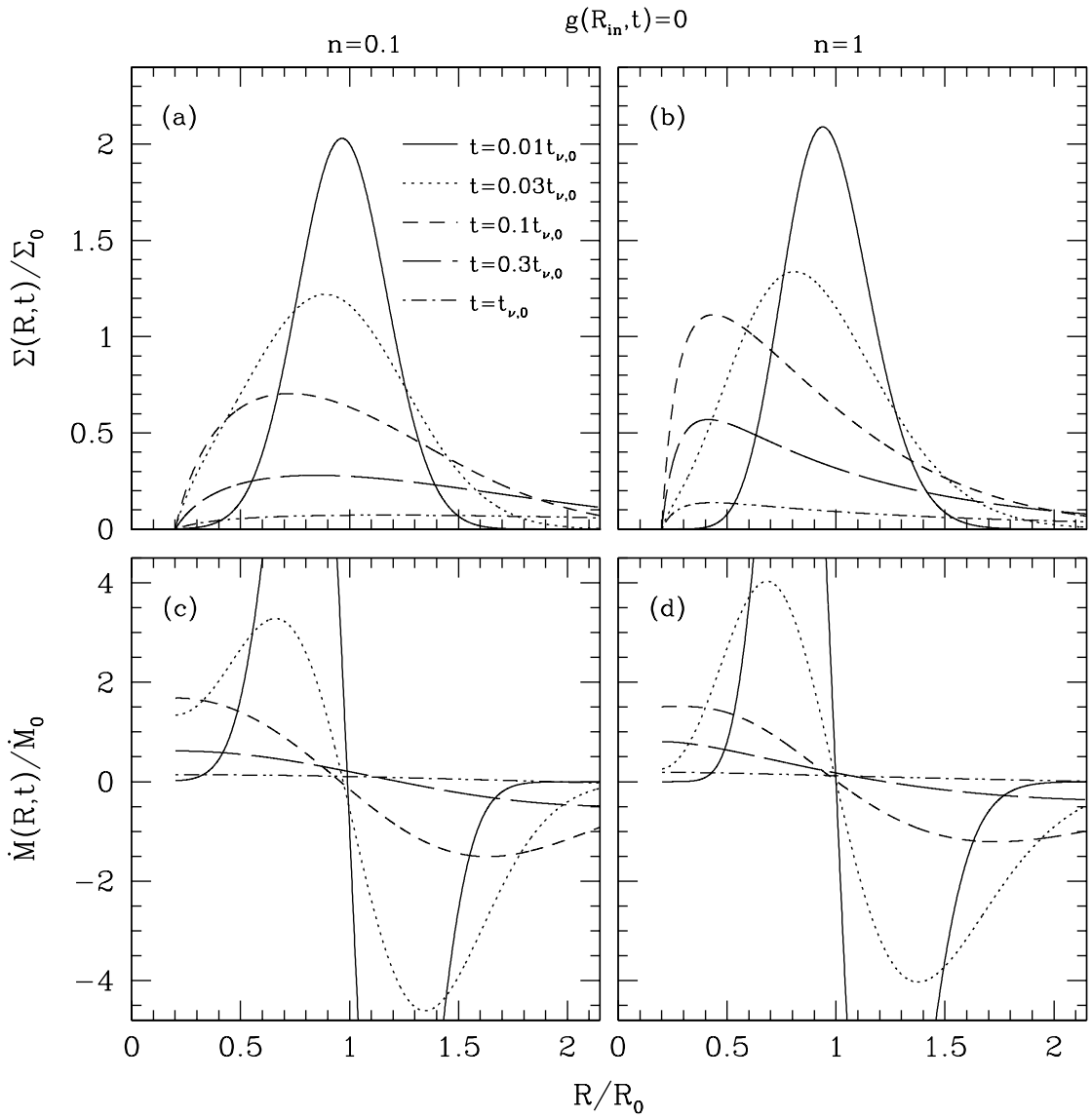

Fig. 3.— Same as as Figure 1, except that the zero-torque boundary condition is applied at a finite radius $R_{\rm in} = R_0/5$. As gas flows near the inner boundary, it exhibits the well-known behavior $\Sigma \propto R^{-n}(1-\sqrt{R_{\rm in}/R})$ of LP74.

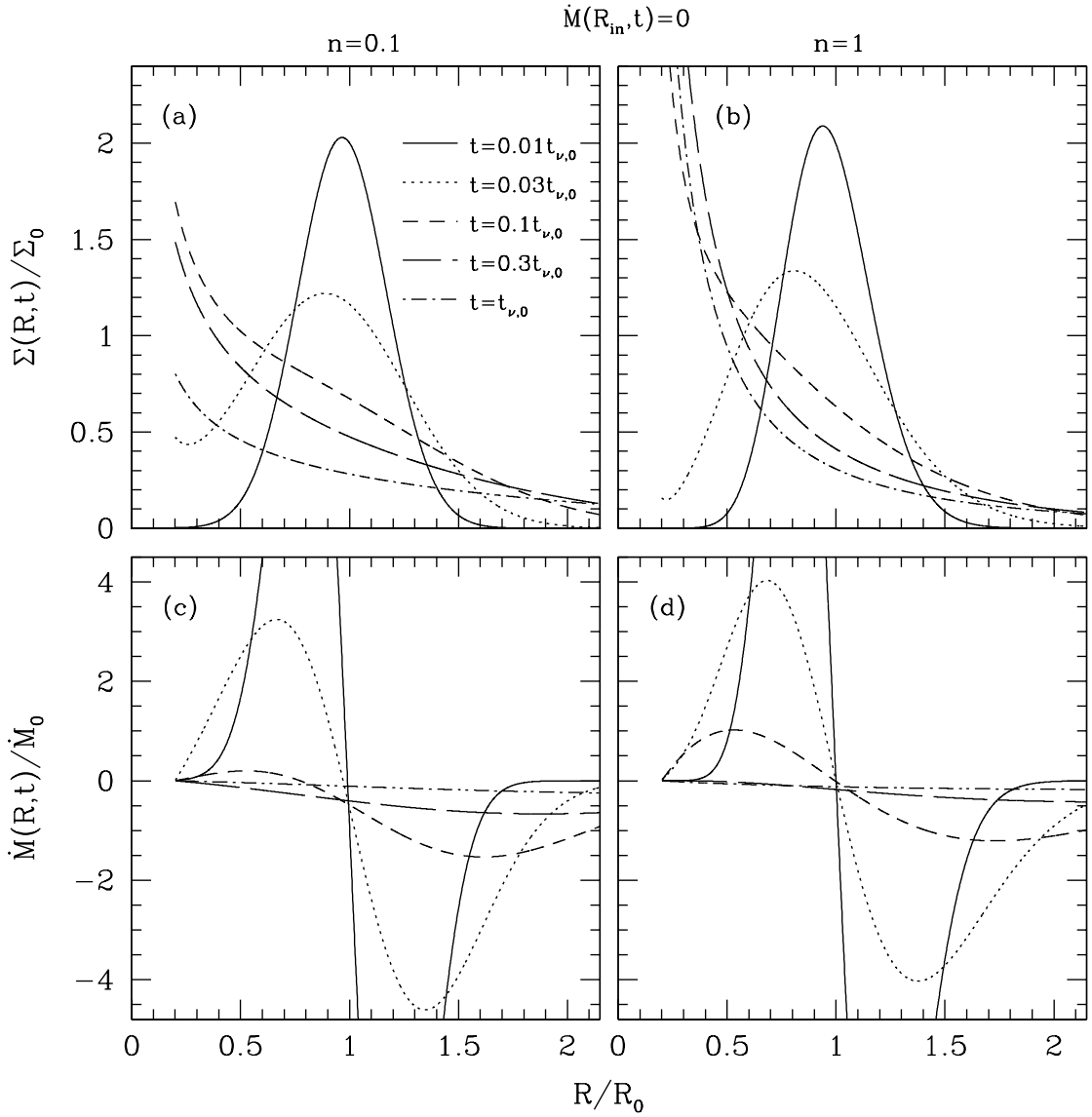

Fig. 4.— Same as as Figure 2, except that the zero-flux boundary condition is applied at a finite radius $R_{\rm in} = R_0/5$. Note that the $n = 1$ case was solved analytically by Pringle (1991).